Molecular Genetics and Metabolism Reports 41 (2024) 101168

Contents lists available at ScienceDirect

Molecular Genetics and Metabolism Reports

journal homepage: www.elsevier.com/locate/ymgmr

Biallelic variants in the *NDUFAF6* cause mitochondrial respiratory complex assembly defects associated with Leigh syndrome in probands

Yuwei Zhou [a,b,1], Xiaofei Zeng [b,1], Luyi Zhang [b], Xiaojie Yin [b], Xue Ma [c], Keyi Li [b], Peijing Qiu [d], Xiaoting Lou [a,b], Liqin Jin [b,e,*], Ya Wang [b,*], Yanling Yang [c,*], Ting Shen [d,*]

[a] *Laboratory Medicine Center, Department of Genetic and Genomic Medicine, Zhejiang Provincial People's Hospital, Affiliated People's Hospital, Hangzhou Medical College, Hangzhou, Zhejiang, China*
[b] *Key Laboratory of Laboratory Medicine, Ministry of Education, Zhejiang Provincial Key Laboratory of Medical Genetics, School of Laboratory Medicine and Life Sciences, Wenzhou Medical University, Wenzhou, Zhejiang, China*
[c] *Department of Pediatrics, Peking University First Hospital, Beijing, China*
[d] *Eye Center, the Second Affiliated Hospital, Zhejiang University School of Medicine, Hangzhou, Zhejiang, China*
[e] *Department of Scientific Research, Zhejiang Provincial People's Hospital, Affiliated People's Hospital, Hangzhou Medical College, Hangzhou, Zhejiang, China*

ARTICLE INFO

Keywords:
Mitochondrial disease
Leigh syndrome
Complex I deficiency
NDUFAF6

ABSTRACT

Background: Variants in *NDUFAF6* have been reported to be associated with Leigh syndrome. However, further expansion of the *NDUFAF6*-phenotype and variants spectrum of *NDUFAF6*-related Leigh syndrome are still required.

Methods: Two patients diagnosed with Leigh syndrome were recruited, and whole-exome sequencing was performed to identify the genetic variants responsible for the abnormal gait, dystonia, and bilateral basal ganglia lesions, followed by validation using Sanger sequencing. Detailed medical records of the patients were collected and reviewed. Patient-derived immortalized B lymphocytes were generalized for functional assays. The clinical manifestations of the patients in this study and previously reported studies are summarized.

Results: Two patients developed gait dystonia followed by rapid progression to generalized dystonia and psychomotor regression. Brain magnetic resonance images showed lesions in bilateral symmetric basal ganglia. We identified that patient 1 and patient 2 had two missense changes (NM_152416 c.371 T > C, c.923 T > C and c.371 T > C, c.920 A > T) in *NDUFAF6*, respectively. The deficiency of mature super complex of complex I was confirmed in patient-derived immortalized B lymphocytes. Meanwhile, cellular ATP production was decreased, and mitochondrial ROS was increased. A literature review of 18 patients carrying variants in *NDUFAF6* was conducted, focusing on neurological presentation.

Conclusions: *NDUFAF6*-related Leigh syndrome is a relevant cause of initial symptoms with abnormal gait, dystonia, and bilateral basal ganglia lesions. Two novel genetic variants, c.923 T > C and c.920 A > T were reported, which expands *NDUFAF6*-related Leigh syndrome and is advantageous for genetic counseling.

1. Background

Leigh syndrome (LS, OMIM 256000) is the most common subtype of mitochondrial disease observed in pediatric patients, characterized by impaired mitochondrial oxidative phosphorylation (OXPHOS) system functions [1]. The clinical manifestation of LS is highly heterogeneous, as specified by psychomotor retardation, dystonia, ataxia, encephalopathy, and neuroradiologic presentation such as bilateral symmetric lesions in the basal ganglia, brain stem or other central nervous system regions, which leads to the diagnosis of LS depending on typical clinical presentation and definite pathogenic genes [2,3]. Fabian Baertlin [3] et al. suggested that LS be defined in terms of the three most prevalent and distinguishing aspects: a. neurodegenerative diseases; b. mitochondrial dysfunction caused by inherited genetic defects; c.

Abbreviations: LS, Leigh syndrome; OXPHOS, oxidative phosphorylation; CI, complex I; CII, complex II; CIII, complex III; CIV, complex IV; CV, complex V; MRI, Magnetic Resonance Imaging FLAIR: fluid attenuated inversion recovery.

* Corresponding authors at: Ting Shen, Eye Center, the Second Affiliated Hospital, Zhejiang University School of Medicine, Hangzhou, Zhejiang, China.
E-mail address: medicat@zju.edu.cn (T. Shen).

[1] Authors contributed equally to this work.

https://doi.org/10.1016/j.ymgmr.2024.101168
Received 28 May 2024; Received in revised form 21 September 2024; Accepted 27 November 2024

accompanied by bilateral central nervous system lesions. When these criteria are only partially met or patient present with unusual symptoms or imaging features, Leigh-like syndrome should be taken into consideration. Meanwhile, LS has a high mortality rate. Patients with early-onset LS have more severe presentations than late-onset type and the median age at death was 2.4 years [2,4,5]. Most patients died of central respiratory dysfunction. Collectively, it is still necessary to improve early accurate diagnosis rate and prenatal screening by establishing the correlation between genotype and clinical phenotype of LS.

NDUFAF6 (NADH: ubiquinone oxidoreductase complex assembly factor 6), also referred to as *C8orf38*, was mined and identified as a respiratory chain complex I (CI) assembly factor by phylogenetic profiling and homozygosity mapping in two siblings diagnosed with LS [6]. NDUFAF6 was involved in the early stage of the CI assembly process [6,7]. It also plays a role in the assembly, assembly, and maturation of CI [7]. CI is the largest complex in mitochondrial OXPHOS systems and acts as the starting point of the whole reaction. Cells that require a lot of energy are more susceptible to a shortage in CI, like neurons [8]. The assembly and maturity of OXPHOS complexes are an intricate and multi-step process, which comprise multifarious proteins that are categorized as core proteins and assistant proteins. CI deficiency is the most common respiratory chain defect in human disorders [9,10]. The intermediate for OXPHOS complexes assembly is called "respirasome" or respiratory chain super complex.

Here, we sorted out two patients' clinical, biochemical, and genetic information and confirmed the defective assembly of respiratory super complex in patient-derived immortalized B lymphocyte cells. The spectrum of pathogenic variants in *NDUFAF6* was broadened with the discovery of two variants.

2. Material and method

2.1. Patient recruitment and ethics approval

Patients were recruited by the Department of Pediatrics, Peking University First Hospital. Our study was approved by the Ethics Committee of Peking University First Hospital (2017–217).

2.2. Cell lines and culture conditions

B95–8 cell line (Female; RRID: CVCL_1953) was obtained from Cell Bank of the Chinese Academy of Science (Shanghai, China). Cell lines mentioned above have been authenticated by short tandem repeat (STR) profiling identification. Human peripheral blood-derived immortalized B lymphocytes were constructed by our lab.

The generation of immortalized B lymphocytes was described previously [11]. Mononuclear cells were isolated from the patient peripheral blood by lymphocyte separation medium (Solarbio, Beijing, China), and the B lymphocytes were infected with Epstein-Barr virus obtained from B95–8 cells [12] supplemented with 0.5 mg/mL phytohemagglutinin (Sigma-Aldrich) and 1 mg/mL cyclosporin A (Sigma-Aldrich).

Immortalized B lymphocytes were cultured in Roswell Park Memorial Institute (RPMI) 1640 medium (Thermo Fisher Scientific, Waltham, MA, USA, Cat# R6504) with 10 % (*v*/v) fetal bovine serum (Sigma-Aldrich, St. Louis, MO, USA Cat# F8318). The cells mentioned above were cultured in a CO_2 incubator (Thermo Fisher Scientific, Cat# 360) at 37 °C under 5 % CO_2.

2.3. DNA amplification and variants analysis

The DNA was extracted from patient-derived lymphocytes. The targeted sequence was amplified with the primers (Forward-1: 5′-GGCCATTCTTAGTAGTGAGTGAGG-3′; Reverse-1: 5′-ACACTGAGAGCAAGTCTCCC-3′; Forward-2: 5′-AGGCCAGGCAAACGTGATTT-3′; Reverse-2: 5′-GTCCCACGGCAACTTCTCAA-3′) by using Taq Plus Master Mix II (Vazyme, Nanjing, China, Cat# P213). The amplified DNA was sent for Sanger sequencing.

2.4. Blue-native PAGEand immunoblotting

Blue-native PAGE was done according to a described protocol as before [13]. The OXPHOS-super complexes in the native state were lysed with a detergent of 1 % (*v*/v) digitonin (Sigma-Aldrich, Cat# 300410) supplemented with 1 mM PMSF (Sigma-Aldrich). The lysate was homogenized by pipette on ice for 20 min and was separated by centrifugation at 20,000 *g* for 20 min later. The supernatant was removed and was quantified by Pierce BCA Protein Assay Kit (Thermo Fisher Scientific). The blue-native PAGE gel with a concentration gradient of 3 %–11 % for mitochondrial super complex assay. The solubilized proteins were separated by a 3 %–11 % gradient gel in Cathode buffer B/8 (containing 0.0025 % anionic dye Coomassie blue G-250, Sigma-Aldrich, Cat# 115444) in electrophoresis procedures. The whole experiment was processed at 4 °C or on ice and all electrophoresis fluids, reagents, and other materials were pre-cooled.

For immunoblotting, the protein was electroblotted onto 0.22 μM PVDF membrane (Bio-Rad, Hercules, CA, USA, Cat# 1620177). After blocking with 5 % non-fat milk for 1 h at room temperature, membranes were incubated with appropriate primary antibodies at 4 °C overnight. Following incubation, the blot was washed 3 times with TBST and incubated with reaction-specific secondary antibodies. The Blue-native PAGE blots were detected by alkaline phosphatase (AP)-based colorimetric reaction. Regarding the AP reaction, the membranes were incubated in solution with 0.4 mg/mL NBT (Sigma-Aldrich, Cat# N6876) and 0.2 mg/mL BCIP (BBI Life Science, A610072–0500) in AP buffer (0.1 M Tris-HCl, 0.1 M NaCl, 10 mM $MgCl_2$, pH = 9.5). The OXPHOS super complexes were detected using the primary antibodies as follows: anti-Grim19 (1:1000, Abcam, Cambridge, CB2 0AX, UK, Cat# 110240), anti-SDHA (1:3000, Abcam, Cat# ab14715), anti-UQCRC2 (1:2000, Abcam, Cat# ab14745), anti-MTCO1 (1:2000, Abcam, Cat# ab14705), anti-ATP5A (1:3000, Abcam, Cat# ab14748). TOM70 (1:2000, Proteintech, Cat# 14528–1-AP) was used as an internal loading control. Secondary antibodies as follows: Anti-rabbit IgG, HRP-linked antibody (Cell Signaling Technology, Cat# 7074), Anti-mouse IgG, HRP-linked antibody (Cell Signaling Technology, Cat# 7076), Anti-mouse IgG, AP-linked antibody (Cell Signaling Technology, Cat# 7056).

2.5. Cellular ATP production

The production of the whole cell was identified by ATP bioluminescent somatic cell assay kit (Thermo Fisher Scientific) following the protocol provided by the manufacturer. In brief, cells were extracted by a solution consisting of 100 mM Tris-base and 4 mM EDTA-Na_2 (pH = 7.75). The reaction system is contained with 5 μL Reaction Buffer, 0.025 μL Luciferase, 10 μM DTT, and 10 mM D-luciferin diluted water to 100 μL. Then resuspended mixed solution were added to the plate. Light emission at 560 nm was measured using a SpectraMax iD3 Multi-Mode Microplate Reader (Molecular Devices, Shanghai, China).

2.6. Mitochondrial ROS production

The amount of mitochondrial ROS was measured with MitoSOX Red mitochondrial superoxide kit (Thermo Fisher Scientific) according to the manufacturer's instructions. Cells were collected by Hank's Balanced Salt Solution (HBSS, Thermo Fisher Scientific) buffer and resuspended by working solution with 5 μM MitoSOX red reagent diluted by HBSS buffer. The mixture was incubated at 37 °C for 10 minuntes. Finally, the fluorescence signal was evaluated by flow cytometry.

2.7. Quantification and statistical analysis

All quantitative experiments were performed with three independent replicates, and all quantitative data are represented as mean ± SEM. Graphs were generated by Prism 10.0. Comparisons of means between the groups were performed with one-way ANOVA (GraphPad Software, San Diego, CA, USA).

3. Results

3.1. Case presentation

Patient 1 (P1), at the age of 3-year-7-month old, was admitted to a local hospital due to walking instability for more than 1 month. The X-ray examination of both lower limbs showed no abnormality. The presence of cerebral palsy and metabolic encephalopathy could not be ruled out, leading to patient referral to our hospital. The patient birth history was normal with full-term delivery and denied perinatal hypoxia. The patient birth weight was recorded as 3350 g. At the age of 3-year-4-month old, the patient had intermittent flu. Following a fall, the patient began to walk instability with a scissor gait and decreased exercise tolerance. Subsequently, the patient had motor and language regression presented with not walking alone and slurred speech. At the age of 4 years and 9 months, the patient's verbal expression was generally articulate and coherent, with occasional stuttering. The patient's physical abilities include the ability to stand, roll over, and crawl. However, he was unable to walk independently and highly relies on support, accompanied by exhibits of knee hyperextension and foot eversion. At the age of 4 years and 11 months, the patient's limb issues progressively deteriorated, resulting in an inability to walk alone and necessitating the need for support for standing. At the age of 6-year-3-month old, the patient had frequent headaches and abdominal pain, and vomiting for nearly a week. When the patient is excited, twisting movements and abnormal postures in the body.

Patient 2 (P2), a 2-year-old boy, was referred to the hospital due to developmental delay and ataxic gait. The patient was delivered at full term without any complications throughout the pregnancy and perinatal period with a birth weight of 3100 g. The patient's mother previously had a pregnancy that was terminated the initial pregnancy at 11 weeks gestation due to developmental arrest, which indicated the presence of sex chromosome abnormalities (47, XXY). Additionally, the patient is prone to developing dermatitis. At the age of 14 months, the patient could stand and walk with assistance. The patient, aged 1 year and 9 months, was exhibiting delayed gross motor development. Furthermore, the patient's capacity to engage in physical activities decreased, and his limb problems worsened with time. The patient experienced difficulties with unsteady walking and a lack of coordination of his stride. In addition, the patient also exhibited difficulties in supporting their body weight on their right side, leading to a propensity to stumble or lose balance while jogging. Additionally, his manual dexterity is impaired exhibiting little flexibility and coordination. The patient had feet eversion, characterized by the outward deviation of the lesser toes. The patient exhibits a propensity for frequent falls during running, accompanied by a forward inclination of the body. In addition, his muscle tone instability in all four limbs, as well as hyperactivity in the tendon reflexes. The individual possesses the ability to comprehend basic spoken expressions and is capable of identifying colors and rudimentary pictures. The patient exhibits a language developmental delay, characterized by the use of shortened sentences and basic vocabulary. In addition, his speech development is markedly delayed, with just 2–3 meaningful pronunciations.

3.2. Neuroimaging and laboratory tests

A variety of laboratory tests and imaging examinations were conducted on both patients to furnish corroborative proof. Among them, the results of P1 were examined as follows. The laboratory tests in P1 revealed blood lactate concentration of 2.82 mmol/L (range, 0.5–2.2 mmol/L) and pyruvate levels of 116 μmol/L (range, 20–100 μmol/L), β-hydroxybutyric acid levels of 0.49 mmol/L (range, 0.02–0.27 mmol/L), creatine kinase levels of 184.00 U/L (range, 38.00–174.00 U/L), and CK-MBlevels of 27.3 U/L (range, 0.0–24.0 U/L). The results of electrocardiography and echocardiography were within normal parameters. No obvious abnormality in the urine organic acid examination. Due to a suspected brain pathology, no evident anomalous signal was observed in the remaining brain tissue, and a distinct contrast between the grey and white matter was observed. The midline structure did not experience any displacement. There were no notable abnormalities seen in the brainstem or cerebellar hemispheres. To further discern diseases that may manifest lesions of symmetric basal ganglia, we additionally conducted MR spectroscopy, which revealed typical levels of *N*-acetylaspartate, choline, creatine, and lipids, and a lactate peak noted at 1.33 ppm. The presence of a prominent lactate peak suggests the occurrence of acute mitochondrial dysfunction. Based on the observed clinical manifestations, we have deduced that P1 had the potential incidence of LS **(**Fig. 1A-B**)**.

The laboratory test in P2 revealed a lactic acid level of 3.00 mmol/L (range, 1.33–1.78 mmol/L) and β-hydroxybutyrate levels of 0.72 mmol/L (range, 0.02–0.27 mmol/L), LDH levels of 263.61 U/L (range, 120–250 U/L), creatine kinase levels of 168.48 U/L (range, 50–310 U/L), and creatine kinase isoenzyme levels of 19 U/L (range, 0–25 U/L). The other laboratory test results, including serum amino acid analysis, and acylcarnitine were all within normal ranges. Additionally, Magnetic Resonance Imaging (MRI) was conducted on P2. The bilateral cerebral hemispheres exhibited symmetrical characteristics, with a noticeable contrast between grey and white matter. Additionally, symmetrical long T1 and long T2 signals were observed in the basal ganglia on both sides. The T2-fluid attenuated inversion recovery (FLAIR) sequence exhibited areas of increased signal intensity, restricted diffusion, heterogeneous internal signal, and a combination of high and low signal intensities. These findings were predominantly observed in the caudate nucleus and putamen regions. Based on the clinical manifestations, it was deduced that P2 had been diagnosed with LS **(**Fig. 2**)**.

3.3. Characterization of NDUFAF6 variants

To further clarify the pathogenic molecular genes, the whole exome sequence and mitochondrial DNA sequence were performed with blood samples of two patients, respectively. According to the criteria mentioned before [14,15], the sequencing result of P1 indicates, two biallelic variants in *NDUFAF6* (NM_152416) c.371 T > C (p.Ile124Thr) and c.923 T > C (p.Ile308Thr) were identified and verified by Sanger sequence **(**Fig. 3A**)**. Meanwhile, two biallelic variants in *NDUFAF6* (NM_152416) c.371 T > C (p.Ile124Thr) and c.920 A > T (p.Asp307Val) were identified and then verified by the Sanger sequence in P2 **(**Fig. 3B**)**.

To further dissect the pathogenicity of the above two variants, we queried a series of bioinformatics analyses. As shown in Fig. 3C, the allele frequency of c.371 T > C and c.923 T > C in gnomAD was extremely low (0.00003, 0.00009), in ExAc was also low (0.00007 and 0.00004). the allele frequency of c.371 T > C in 10,000 genomes is 0.0002. The variant c.920 A > T has not been previously documented in the genome aggregation database, and there is no known association with human disease. The pathogenicity of variants predicted by silico analysis (SIFT and MutationTaster), resulting that c.371 T > C, c.920 A > T, and c.923 T > C might be deleterious and disease-causing, respectively. Both p.I124, p.D307, and p.I308 were highly conserved among species suggesting they are important for the function of NDUFAF6 protein **(**Fig. 3D**)**.

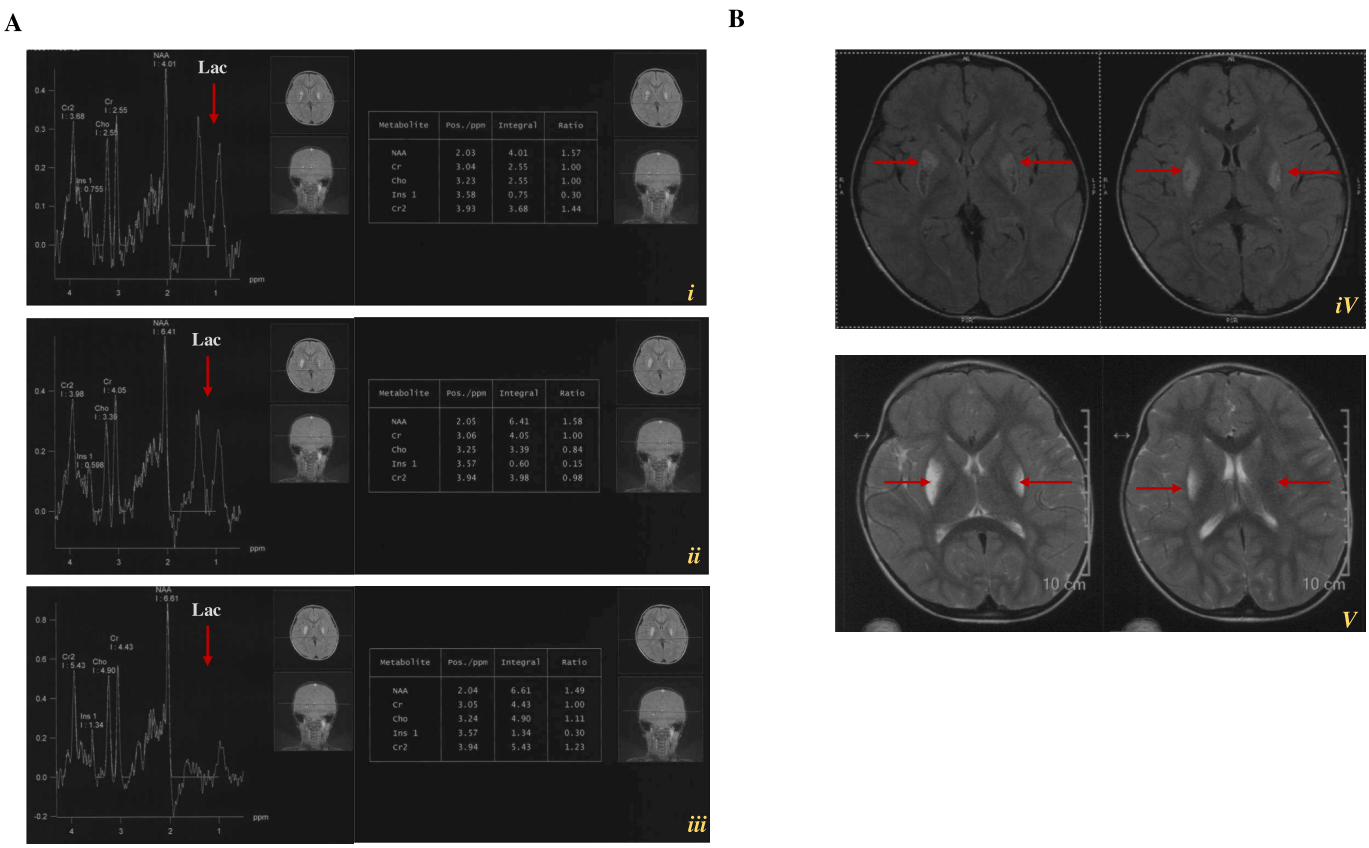

Fig. 1. Brain imaging manifestations of Patient 1.
A. Magnetic resonance spectrum (MRS) showed a broad inverted lactate peak (marked with a red arrow). **B.** Brain magnetic resonance imaging on T1-weighted imaging (T1WI) and high signal on T2-weighted imaging (T2WI) of Patient 1.

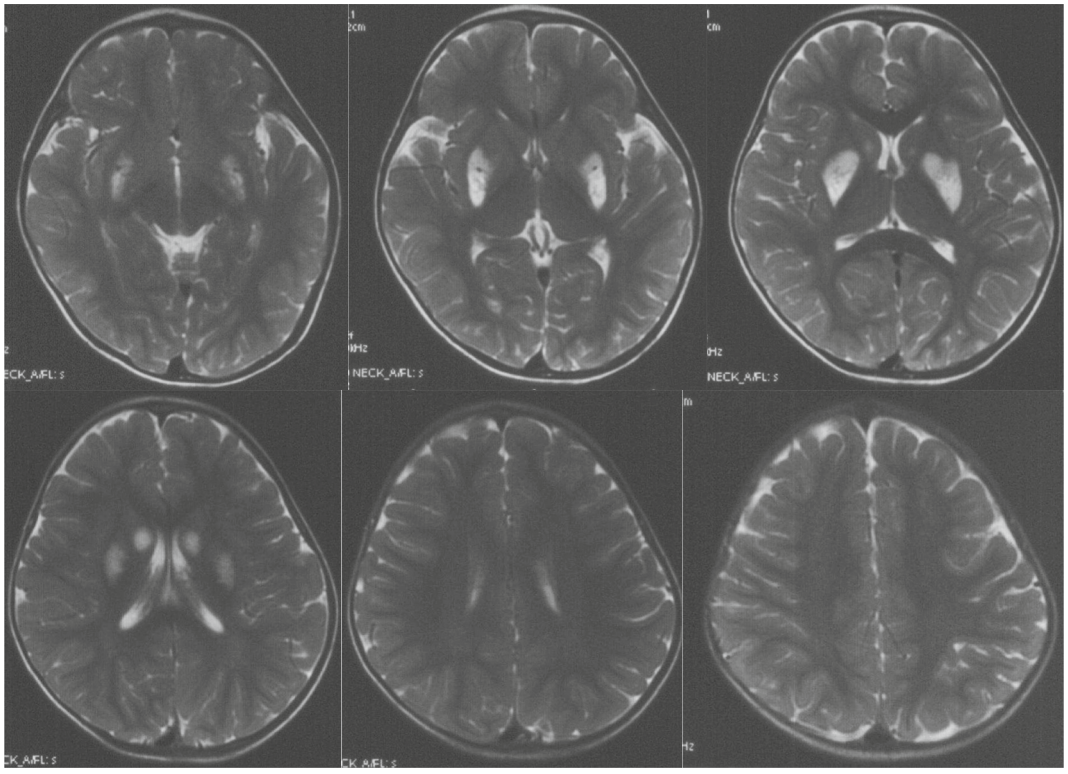

Fig. 2. Brain imaging manifestations of Patient 2.

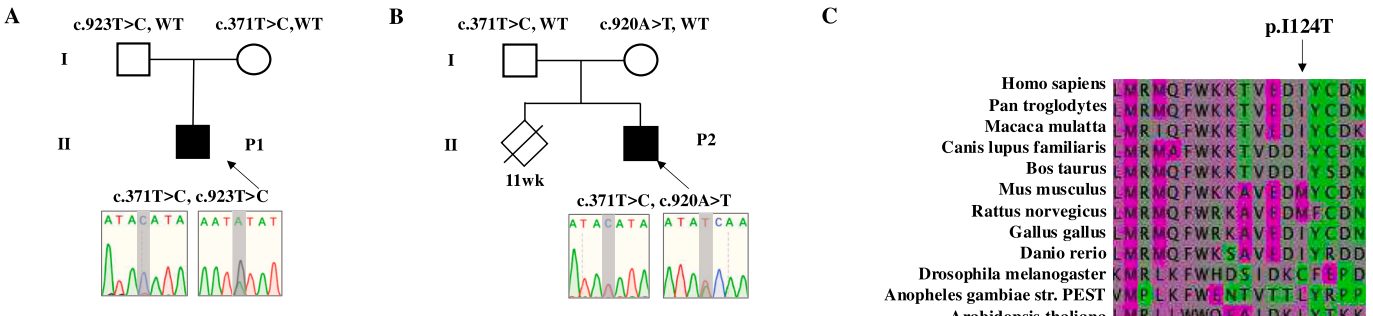

D

Nucleotide Change / Amino acid Change	c.371T>C p.IIe124Thr	c.920A>T p.Asp307Val	c.923T>C p.I308T
Allele frequency in 1000 genomes	0.00020	NA	NA
Allele frequency in gnomAD	0.00003	NA	0.00009
ExAc allele frequency	0.00007	NA	0.00004
dbSNP	rs201732170	NA	rs368450784
Clinvar	VUS	NA	NA
HGMD	Pathogenic	NA	NA
SIFT	Deleterious	Deleterious	Deleterious
MutationTaster	Disease causing	Disease causing	Disease causing
ACMG	Likely pathogenic	Likely pathogenic	VUS

Fig. 3. *NDUFAF6* variant features.
A-B. Pedigree of affected individuals. Squares indicate males and a circle for females. Arrows indicated for proband. WT, wild type. Variants were identified by the Sanger sequencing.
C—D. *In silico* and conservation of amino acids analysis of *NDUFAF6* variants: conservation of amino acids in mammals and pathogenicity prediction and allele frequency of three variants. NA, not available.

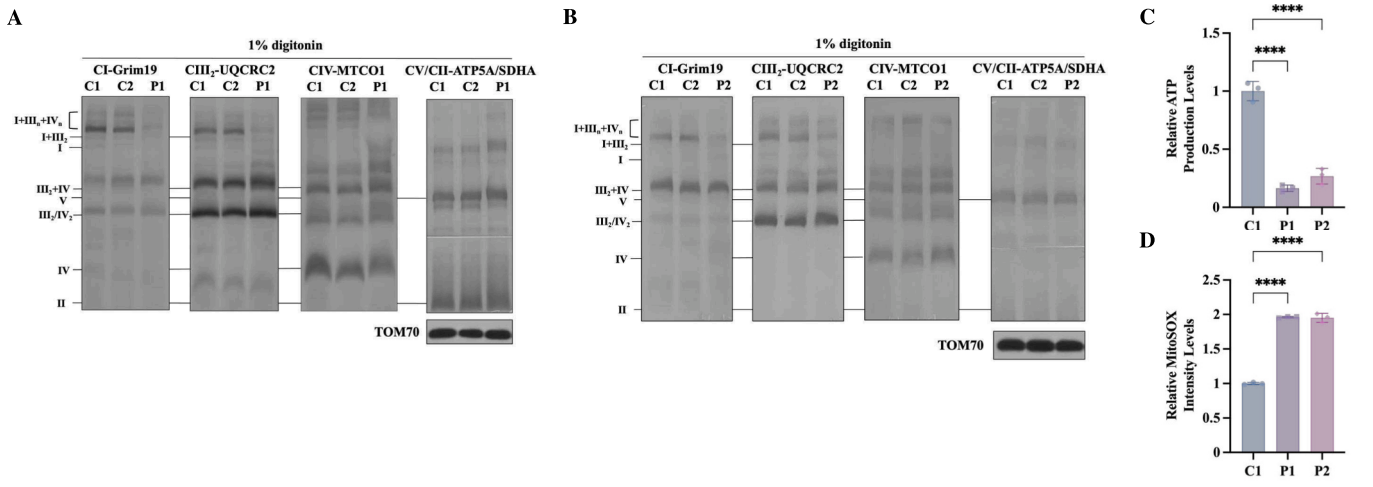

Fig. 4. *NDUFAF6* mutations alter mitochondrial OXPHOS function.
A-B. Blue-native PAGE and immunoblotting analysis of mitochondrial OXPHOS super complexes (SC). Digitonin-solubilized protein was separated by 3 %–11 % blue-native PAGE and the SC was immunoblotting with anti-Grim19, anti-SDHA, anti-UQCRC2, anti-MTCO1 and anti-ATP5A antibodies (showed as CI, CII, $CIII_2$, CIV and CV), respectively. C1 and C2 were healthy controls. TOM70 was used as an internal loading control.
C. Cellular ATP production in immortalized lymphocytes from the patients and healthy control (C1) was normalized to protein concentration.
D. Production of mitochondrial superoxide in immortalized lymphocytes from the patient and healthy controls (C1).

3.4. Variants in NDUFAF6 impaired hole-CI independent super complex assembly

To further clarify the role of *NDUFAF6* in the assembly of mitochondrial respiratory chain super complexes *in vivo*, the immortalized B lymphocytes were generated from two patients. Blue-native PAGE analysis followed by immunoblotting of OXPHOS super complexes from digitonin-solubilized cell lysates showed a deficiency of mature CI and an accumulation of incomplete assembly CI, indicating the failure of CI assembly in patient-derived lymphocytes. These results confirm that NDUFAF6 is indispensable for CI assembly and OXPHOS functions (Fig. 4A-B). Full-length blots are presented in Supplementary Figure. The cells from P1 and P2 carried variants of *NDUFAF6* led to a significant decrease in cellular ATP content compared with the matched control cell (Fig. 4C). Consistently, the cells from P1 and P2 resulted in more mitochondrial superoxide content than that in control cells (Fig. 4D).

4. Discussion

LS, as a type of multi-system disease involvement, is a challenge in clinical diagnosis [16]. In the clinic, the diagnosis of complicated diseases more likely depends on clinical presentation-oriented gene panels for genetic confirmation. The development and application of next-generation sequencing have provided considerable advancement in determining the molecular pathogenesis of heterogeneous diseases. However, in the process of diagnosis of rare diseases, depending merely on clinical features, misdiagnosis is not uncommon, especially in affected patients who have not undertaken genetic sequence testing. Thus, the spectrum of variants is intensively required for expansion. In this study, we have reported 2 patients presented with the typical syndrome of LS harboring compound heterozygous variants in the *NDUFAF6* gene for the expansion of LS-associated pathogenic genes and variants.

The suspicion and diagnosis of mitochondrial disease or subtype of it were based on clinical presentation, biochemical tests, and neuroimaging studies. In this study, the patients manifested dystonia and abnormal gait as the initial symptoms in childhood. Gradual progression of symptoms led to developmental delay and patients were observed including elevated lactic acid in serum. LS is characterized by the presence of bilateral symmetrical necrotizing lesions in the brainstem, basal ganglia, thalamus, and spinal cord, which is consistent with the phenotype of patients with basal ganglia lesions [17]. Lebre et al. reported that the commonly exhibited brain MRI findings in patients with CI deficiency were bilateral symmetrical brainstem lesions, abnormalities in at least one striatum, and lactate peaks on MRS, which were more prevalent than other complex defects. In particular, we noted that patient 1 presented a late-onset LS [18]. LS is traditionally considered to be an infancy and early childhood onset disease that occurs before the age of 2 years. Most cases, over 50 %, are typically detected in patients who are less than 1 year old. The occurrence of late-onset LS is infrequent. Based on prior literature, it has been observed that characteristic indications and manifestations may manifest in cases of late-onset LS. Late-onset LS is characterized by a range of symptoms including intellectual deterioration, vertical gaze paralysis, headache, memory loss, and visual hallucinations, which is partly consistent with the phenotype of patient 1 with intellectual decline and frequent headaches.

At present, the phenotype-driven panel could efficiently obtain a genetic diagnosis. Still, the application depends on the completeness of the correlation between clinical phenotype and genotype, which ensures that the true pathogenic gene is included in the screening panel. Therefore, expanding the pathogenic gene spectrum and clinical phenotype and genotype spectrum, not just for LS, is essential. LS is genetically heterogeneous and encoded by two genomes (mitochondrial and nuclear). Pathogenic mutations in more than 95 genes have been identified [19–22], with LS caused by CI defects accounting for 35 % ~ 50 % of reported cases. In 2008, Pagliarini reported the first case diagnosed with LS caused by *NDUFAF6* [6]. Up to now, 18 patients with variants in *NDUFAF6* (Fig. 5, Table 1), of which the most variations are reported in exon 2 [6,23–29]. The imperative to not overlook the further exploration of LS-harmful genes and variants is of utmost importance. In our study, to ascertain the causative gene responsible for the patient presentations and explore the potential existence of gene-expanding, massively parallel sequencing was performed, which identified the previously reported missense change c.371 T > C and two novel missense change c.923 T > C and c.920 A > T variant in the *NDUFAF6* in two patients, respectively.

Successful assembly of CI requires assistance from more than 10 assembly factors, of which *NDUFAF6* was recently identified as a mitochondrial inner membrane factor faced to the matrix important for the integration of ND1 into an early-stage assembly intermediate [30]. Lack of *NDUFAF6* led to a sharp decrease in CI and assembly failure of holo-CI. In the present study, we confirmed the essential role of *NDUFAF6* in the assembly of CI and the operation of OXPHOS function in patient-derived immortalized lymphocyte cells by blue-native PAGE. This impairment in assembly could potentially contribute to the manifestation of LS.

In summary, two Chinese patients were recorded *NDUFAF6*-related Leigh syndrome as a relevant cause of childhood-onset dystonia and bilateral basal ganglia lesions. And one patient presented with rare symptoms of late-onset LS. Two novel genetic variants, c.923 T > C and c.920 A > T, in *NDUFAF6*-related LS were reported.

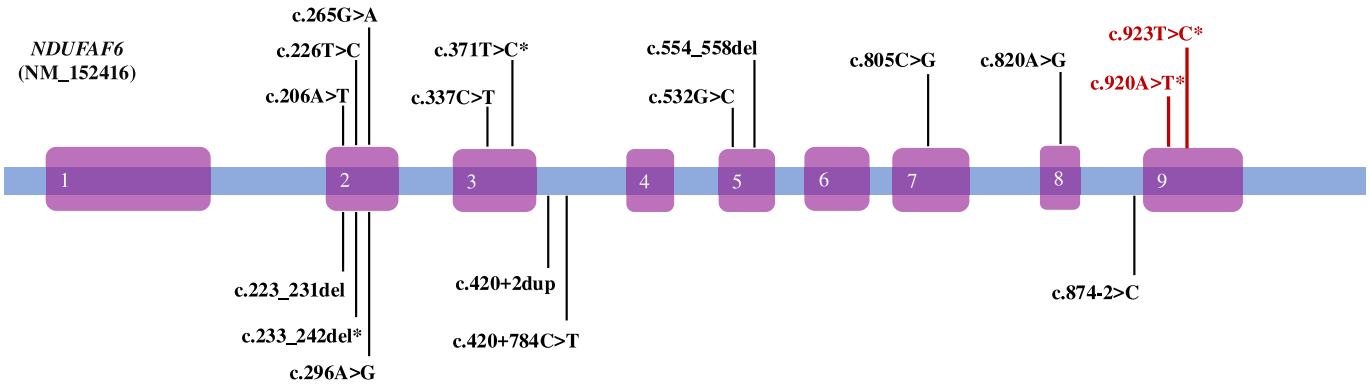

Fig. 5. The genetic spectrum of *NDUFAF6*.
Pathogenic variants reported of *NDUFAF6* are collected. Asterisks denote novel variants.

Table 1
Variants and neurological features of patients with *NDUFAF6*-related Leigh syndrome.

	This study		Pagliarini 2008		Bianciardi 2016	Kohda 2016			
Mutations	c.371 T > C, c.923 T > C	c.371 T > C, c.920 A > T	c.296 A > G (hom)	c.296 A > G (hom)	c.532G > C (hom)	c.371 T > C, c.805C > G	c.820 A > G (hom)	c.226 T > C, c.805C > G	c.206 A > T, c.371 T > C
Age at onset	43 months	14 months	10 months	7 months	42 months	72 months	17 months	At birth	2 months
Clinical features Onset	walking instability	developmental delay and ataxic gait	Focal right hand seizures, ataxia, rigidity, decreased movement and strength	Focal right hand seizures, ataxia, rigidity, decreased movement and strength	Insidious, gross motor and language difficulties, dystonic movements and decreased fine motor ability	NA	NA	NA	NA
Neurological presentation	walk instability with a scissor gait and decreased exercise tolerance,vomit, motor and language regression, frequent headaches	uncoordinated stride and eversion of the feet, limited weight-bearing capacity, frequent falls, language developmental delay	Focal right-hand seizures, ataxia, rigidity, decreased movement and strength	Focal right-hand seizures, ataxia, rigidity, decreased movement and strength	Dysarthria, dystonic movements, decreased fine motor abilities, dystonia	NA	NA	NA	NA
Sex	Male	Male	Female	Male	Male	Male	Male	Female	Male
Lactate in plasma	Elevated	Elevated	Elevated	Elevated	Normal	NA	NA	Elevated	NA
Brain MRI	symmetrical low signal on T1-weighted imaging (T1WI) and high signal on T2-weighted imaging (T2WI), fluid-attenuated inversion recovery (FLAIR), and diffusion-weighted imaging (DWI) in the bilateral posterior region of the lenticular nucleus	long T1 and long T2 signals were observed in the basal ganglia on both sides	Neuroimaging presentation consistent with Leigh syndrome	Neuroimaging presentation consistent with Leigh syndrome	Bilateral T2 intensities in putamen, caudate nuclei, dentate nuclei	NA	Abnormalities of the basal ganglia	NA	Abnormalities of the basal ganglia
MRC CI (% of residual activity)	NA	NA	36 % in muscle 14 % in fibroblasts 20 % in liver	14 % in fibroblasts	72 % in muscle 32 % in fibroblasts	<30 % in a fibroblast	<30 % in a fibroblast	<30 % in a fibroblast	<30 % in a fibroblast
Basal ganglia necrosis	bilateral posterior region of the lenticular nucleus	Caudate and putamen	Putamen	Caudate and putamen	Caudate and putamen	NA	NA	NA	NA

	Fang 2017	Catania 2018			Baide-Marena 2019			Johnstone 2020	Kim 2022
Mutations	c. 337C > T, c.265G > A	c.532G > C, c.420 + 784C > T	c.532G > C, c.420 + 784C > T	c.532G > C, c.420 + 784C > T	c.371 T > C, c.554_558delTTCTT	c.371 T > C, c.554_558delTTCTT	c.371 T > C, c.554_558delTTCTT	c.371 T > C, c.420 + 2dup	c.371 T > C, c.233_242del
Age at onset	4 years	21 months	12 months	60 months	30 months	30 months	17 months	4 years	3 years
Clinical features Onset	Movement disorder, abnormal gait, exercise intolerance, weakness, difficulty swallowing, increased muscle tension	Febrile episode and temporary loss of autonomous gait	Insidious, limb dysmetria and trunk titubation	Insidious, gait unsteadiness and motor coordination problems	Insidious, toe walking and speech difficulties	Insidious, toe walking and speech difficulties	Insidious, toe walking and speech difficulties	Febrile episode, and months later toe walking and focal hand dystonia	Left hand clumsiness and frequent falling
Neurological presentation	Bilateral basal ganglia and gradually expand to centrum semiovale	Ataxic gait, fine tremor, dysmetria, drooling, hypertonia, dystonia	Ataxic gait, fine tremor, dysmetria, drooling, hypertonia, dystonia	Drooling, dysarthria, oromandibular dystonia, Extrapyramidal hypertonia, dystonia	Dysarthria, stuttering, dysphagia, dystonia	Dysarthria, stuttering, dysphagia, dystonia	Dysarthria, stuttering, dysphagia, dystonia	Dysarthria, ataxic gait, dystonia	Dystonic, ataxic movements, spastic hypertonia
Sex	Male	Male	Female	Male	Female	Male	Male	Male	Male
Lactate in plasma	Normal	Elevated	Elevated	Normal	Elevated	Elevated	NA	Normal	Elevated
Brain MRI	Kim 2022	T2 hyperintensities in putamen, dentate nuclei and caudate nucleus	Bilateral T2 hyperintensities in dentate nucleus and superior cerebellar peduncle	Bilateral T2 hyperintensitiesin putamen	Bilateral T2 hyperintensitiesin putamen	Bilateral T2 hyperintensities in putamen, and partly in caudate	Bilateral T2 hyperintensities and volume loss in putamen and caudate	Bilateral T2 hyperintensities in the putamina without mass effect or contrast enhancement	T2 hyperintensities in putamen

(*continued on next page*)

Table 1 (*continued*)

	Fang 2017	Catania 2018			Baide-Marena 2019			Johnstone 2020	Kim 2022
Mutations	c. 337C > T, c.265G > A	c.532G > C, c.420 + 784C > T	c.532G > C, c.420 + 784C > T	c.532G > C, c.420 + 784C > T	c.371 T > C, c.554_558delTTCTT	c.371 T > C, c.554_558delTTCTT	c.371 T > C, c.554_558delTTCTT	c.371 T > C, c.420 + 2dup	c.371 T > C, c.233_242del
MRC complex I (% of residual activity)	NA	42 % in muscle 38 % in fibroblasts	NA	Normal	60 % in muscle	Reduced in muscle	Reduced in muscle	126 % in fibroblast	NA
Basal ganglia necrosis	NA	Caudate and putamen	NA	Putamen	Caudate and putamen	Caudate and putamen	Putamen	Putamen	Putamen

NA, not available.

Ethical statements

The Ethics Committee of Peking University First Hospital (2017–217) approved the study.

Patient consent statement.

All voluntary participants have signed informed consent forms in this study.

Funding

This work was supported by the National Natural Science Foundation of China [grant number 82072366, L.J.]; the National Key Research and Development Program of China [grant number 2021YFC2700903, Y.Y.]; Research and Development Plan of Zhejiang Science and Technology Department [grant number 2023C03089, P. Q].

CRediT authorship contribution statement

Yuwei Zhou: Writing – review & editing, Writing – original draft, Methodology, Investigation, Formal analysis, Conceptualization. **Xiaofei Zeng:** Writing – review & editing, Investigation. **Luyi Zhang:** Writing – review & editing, Writing – original draft, Investigation. **Xiaojie Yin:** Writing – review & editing, Writing – original draft, Investigation. **Xue Ma:** Writing – review & editing, Writing – original draft, Visualization, Investigation. **Keyi Li:** Writing – review & editing, Methodology. **Peijing Qiu:** Writing – review & editing, Supervision, Resources, Funding acquisition. **Xiaoting Lou:** Writing – review & editing, Validation, Methodology. **Liqin Jin:** Writing – review & editing. **Ya Wang:** Writing – review & editing, Supervision, Resources. **Yanling Yang:** Writing – review & editing, Validation, Supervision, Methodology, Funding acquisition, Conceptualization. **Ting Shen:** Writing – review & editing, Validation, Supervision, Methodology, Formal analysis, Conceptualization.

Declaration of competing interest

The authors have declared that no conflict of interest exists.

Data availability

The datasets used and/or analyzed during the current study are available from the corresponding author on reasonable request. There was no data need to be deposited for this study and the datasets.

Acknowledgments

We thank all the patients and their families for their participation.

Appendix A. Supplementary data

Supplementary data to this article can be found online at https://doi.org/10.1016/j.ymgmr.2024.101168.

References

[1] S. Rahman, et al., Leigh syndrome: clinical features and biochemical and DNA abnormalities, Ann. Neurol. 39 (3) (1996) 343–351.

[2] J. Finsterer, Leigh and Leigh-like syndrome in children and adults, Pediatr. Neurol. 39 (4) (2008) 223–235.

[3] F. Baertling, et al., A guide to diagnosis and treatment of Leigh syndrome, J. Neurol. Neurosurg. Psychiatry 85 (3) (2014) 257–265.

[4] K. Sofou, et al., A multicenter study on Leigh syndrome: disease course and predictors of survival, Orphanet J. Rare Dis. 9 (2014) 52.

[5] A.Z. Lim, et al., Natural history of Leigh syndrome: a study of disease burden and progression, Ann. Neurol. 91 (1) (2022) 117–130.

[6] D.J. Pagliarini, et al., A mitochondrial protein compendium elucidates complex I disease biology, Cell 134 (1) (2008) 112–123.
[7] B.D. Lemire, Evolution, structure and membrane association of NDUFAF6, an assembly factor for NADH:ubiquinone oxidoreductase (complex I), Mitochondrion 35 (2017) 13–22.
[8] N.C. de Souza-Pinto, et al., Mitochondrial DNA, base excision repair and neurodegeneration, DNA Repair (Amst) 7 (7) (2008) 1098–1109.
[9] A. Signes, E. Fernandez-Vizarra, Assembly of mammalian oxidative phosphorylation complexes I-V and supercomplexes, Essays Biochem. 62 (3) (2018) 255–270.
[10] M. Mimaki, et al., Understanding mitochondrial complex I assembly in health and disease, Biochim. Biophys. Acta 1817 (6) (2012) 851–862.
[11] W. Hammerschmidt, B. Sugden, Genetic analysis of immortalizing functions of Epstein-Barr virus in human B lymphocytes, Nature 340 (6232) (1989) 393–397.
[12] G. Tosato, J.I. Cohen, Generation of Epstein-Barr Virus (EBV)-immortalized B cell lines, Curr. Protoc. Immunol. (2007) 7.22.1–7.22.4.
[13] I. Wittig, H.P. Braun, H. Schägger, Blue native PAGE, Nat. Protoc. 1 (1) (2006) 418–428.
[14] S. Richards, et al., Standards and guidelines for the interpretation of sequence variants: a joint consensus recommendation of the American College of Medical Genetics and Genomics and the Association for Molecular Pathology, Genet. Med. 17 (5) (2015) 405–424.
[15] L.C. Wong, et al., Clinical and laboratory interpretation of mitochondrial mRNA variants, Hum. Mutat. 41 (10) (2020) 1783–1796.
[16] R.N. Lightowlers, R.W. Taylor, D.M. Turnbull, Mutations causing mitochondrial disease: what is new and what challenges remain? Science 349 (6255) (2015) 1494–1499.
[17] M. Gerards, S.C. Sallevelt, H.J. Smeets, Leigh syndrome: resolving the clinical and genetic heterogeneity paves the way for treatment options, Mol. Genet. Metab. 117 (3) (2016) 300–312.
[18] C.M. Hong, et al., Clinical characteristics of early-onset and late-onset Leigh syndrome, Front. Neurol. 11 (2020) 267.
[19] N.J. Lake, et al., Leigh syndrome: one disorder, more than 75 monogenic causes, Ann. Neurol. 79 (2) (2016) 190–203.
[20] M. Schubert Baldo, L. Vilarinho, Molecular basis of Leigh syndrome: a current look, Orphanet J. Rare Dis. 15 (1) (2020) 31.
[21] S.L. Stenton, et al., Leigh syndrome: a study of 209 patients at the Beijing Children's hospital, Ann. Neurol. 91 (4) (2022) 466–482.
[22] K. Sofou, et al., Phenotype-genotype correlations in Leigh syndrome: new insights from a multicentre study of 96 patients, J. Med. Genet. 55 (1) (2018) 21–27.
[23] L. Bianciardi, et al., Exome sequencing coupled with mRNA analysis identifies NDUFAF6 as a Leigh gene, Mol. Genet. Metab. 119 (3) (2016) 214–222.
[24] M. Kohda, et al., A comprehensive genomic analysis reveals the genetic landscape of mitochondrial respiratory chain complex deficiencies, PLoS Genet. 12 (1) (2016) e1005679.
[25] H. Baide-Mairena, et al., Mutations in the mitochondrial complex I assembly factor NDUFAF6 cause isolated bilateral striatal necrosis and progressive dystonia in childhood, Mol. Genet. Metab. 126 (3) (2019) 250–258.
[26] A. Catania, et al., Compound heterozygous missense and deep intronic variants in NDUFAF6 unraveled by exome sequencing and mRNA analysis, J. Hum. Genet. 63 (5) (2018) 563–568.
[27] T. Johnstone, et al., Biallelic variants in two complex I genes cause abnormal splicing defects in probands with mild Leigh syndrome, Mol. Genet. Metab. 131 (1–2) (2020) 98–106.
[28] J. Kim, J. Lee, D.H. Jang, NDUFAF6-related Leigh syndrome caused by rare pathogenic variants: a case report and the focused review of literature, Front. Pediatr. 10 (2022) 812408.
[29] F. Fang, et al., The clinical and genetic characteristics in children with mitochondrial disease in China, Sci. China Life Sci. 60 (7) (2017) 746–757.
[30] M. McKenzie, et al., Mutations in the gene encoding C8orf38 block complex I assembly by inhibiting production of the mitochondria-encoded subunit ND1, J. Mol. Biol. 414 (3) (2011) 413–426.